Imaging subsurface lithological and structural features by resistivity tomography: North Beagle Channel (Tierra del Fuego, Argentina)

Alejandro Tassone[1,*], Melina Santomauro[1], Marco Menichetti[2], María Elena Cerredo[3], Marcela Beatriz Remesal[3], Horacio Lippai[1], Emanuele Lodolo[4], and Juan Francisco Vilas[1]

[1] CONICET - Instituto de Geofísica "Daniel A. Valencio". Departamento de Ciencias Geológicas, Facultad de Ciencias Exactas y Naturales. Universidad de Buenos Aires, Argentina.
[2] Istituto di Scienze della Terra, Università di Urbino. I-61029 Urbino, Italy.
[3] CONICET - Departamento de Ciencias Geológicas. Facultad de Ciencias Exactas y Naturales, Universidad de Buenos Aires, Argentina.
[4] Istituto Nazionale di Oceanografia e Geofisica Sperimentale – Borgo Grotta Gigante, 42/c. 34010 Sgonico. Trieste, Italy.
** tassoneale@yahoo.com.ar*

ABSTRACT

Worldwide, the study of fold and thrust belts and characterization of structures are mainly carried out through superficial geological observations and seismic reflection, as the main geophysical prospecting method. In this study we show how the resistivity method is a useful tool for identification of shallow structures (upper 80 m) when combined with the knowledge of the local geology. This is a relative low cost and easily applicable method, which can contribute to image both lithological boundaries and subsurface structures.

The Andes Fueguinos in the area of the Beagle Channel are characterized by a sequence of NNE-verging thrusts stacks of basement emplaced during the middle Cretaceous-Tertiary Andean orogenesis, combined with a strong left lateral strike-slip component. An electric resistivity survey to obtain a 2D electric resistive tomography (ERT) was carried out in the northern shore of the Beagle Channel, west of Ushuaia, in order to better understand the geometric relationships between the basement and cover units in this part of the thrust belt. The method employed, integrated with a field geological survey, allowed to differentiate the electrical signatures of different thin sheets of the thrust belt, where the major faults are recognized by a decrease in resistivity values and sharp lateral variations. Furthermore, the resistivity section shows a good spatial correspondence with a geological section of the study area, where the continuity of the tectonic boundary between the basement (Lapataia Formation) and synrift units (Lemaire Formation) could be followed at depth.

Key words: electrical resistivity tomography, Fuegian Andes, Argentina.

RESUMEN

En general, el estudio de fajas plegadas y corridas se realiza principalmente por medio de observaciones geológicas de superficie y sísmica de reflexión, como principal método geofísico de

prospección. El empleo del método resistivo, combinado con un conocimiento geológico local, resulta una herramienta útil para la identificación de estructuras someras (hasta alrededor de los 80 m de profundidad). Siendo su aplicación sencilla y de relativo bajo costo, permite detectar tanto contactos litológicos como estructuras subsuperficiales.

Los Andes Fueguinos, en el área del Canal de Beagle, se caracterizan por una secuencia de corrimientos con vergencia al NNE emplazados durante la orogenia Andina del Cretácico medio-Terciario, combinado con una importante componente de desplazamiento de rumbo izquierdo. Para una mejor comprensión de las relaciones geométricas entre el basamento y las unidades de la cobertura sedimentaria en esta parte de la faja plegada y corrida, se ha llevado a cabo un levantamiento eléctrico–resistivo de manera de obtener una tomografía eléctrico–resistiva en dos dimensiones (ERT) en la costa norte del Canal de Beagle, al oeste de la ciudad de Ushuaia. Dicho método fue acompañado por un levantamiento de geología de superficie que permitió diferenciar las respuestas eléctricas de diferentes fajas de corrimiento, donde las fallas principales se reconocen por una disminución en los valores de resistividad y bien definidas variaciones laterales. Asimismo, la tomografía resistiva muestra una buena correspondencia espacial con la sección geológica de superficie del área de estudio, donde la continuidad del contacto tectónico entre el basamento (Formación Lapataia) y las unidades de synrift (Formación Lemaire) puede seguirse en profundidad.

Palabras clave: tomografia de resistividad eléctrica. Andes Fueguinos. Argentina.

INTRODUCTION

Investigation of the complex Mesozoic-Cenozoic evolution of the southernmost Andes has mostly relied on classical field geology, often combined with geophysical surveys (seismic, magnetometric, gravimetric surveys, Lodolo *et al.*, 2003, 2007; Tassone *et al.*, 2005; Peroni *et al.*, 2009, among others), combination which proved to be a powerful tool to achieve closer insights into the geodynamic evolution of the Fuegian region.

A relatively recent geophysical method is the electric resistivity tomography (ERT) which has resulted successful in determining the geometry and some structural features and major lithological characteristics in the first tens to several hundred meters below surface (Caputo *et al.*, 2003, 2007; Demanet *et al.*, 2001; Fazzito *et al.*, 2009; Giano *et al.*, 2000; Griffiths and Barker 1993; Nivière *et al.*, 2008; Nguyen *et al.*, 2007; Spichak *et al.*, 2002; Storz *et al.*, 2000; Wise *et al.*, 2003)

In this contribution we present the results of a 2D ERT survey performed almost normal to major structures in the Bahía Ensenada area, southwestern Tierra del Fuego (Argentina), which are further analyzed and interpreted within the geological context. The study area is mostly blanketed by Quaternary deposits and forests that make difficult and imprecise to define the continuity of lithologies and structures recognized in outcrops. Compressive and strike-slip faults characterize the structural grain in the study area; these faults are the focus of our investigation with the objectives of defining their geometries and kinematics. Although depth limited to the uppermost hundred meters, the ERT is a useful tool to shed some light into the shallow anatomy of complexly deformed regions, especially for defining the most recent active structures affecting the Quaternary cover.

GEOLOGICAL AND TECTONIC OUTLINE

From a structural point of view, the region of the Tierra del Fuego island (Figure 1) can be roughly subdivided into several WNW-ESE trending physiographic provinces (Kranck, 1932; Winslow, 1982; Dalziel and Brown, 1989; Suárez *et al.*, 2000; Olivero and Martinioni, 2001; Menichetti *et al.*, 2008 and references therein). The most internal province lies between the forearc active ocean/continent convergence margin of the Chile trench and the late Miocene accretionary wedge in the Pacific Ocean. It is attached to the southern Tierra del Fuego archipelago along the Beagle Channel area, where the Mesozoic-Cenozoic Fuegian calc-alkaline batholith crops out. The Andean Cordillera comprises the northern shore of the Beagle Channel area, the Navarino Island, the eastern part of the Hoste Island and the southern archipelago; it also includes the metamorphic core complex of the Darwin Cordillera. Here, the oldest rocks, which are the former metamorphic basement of the Fuegian chain, crop out in polydeformed medium to high-grade metasedimentary and metavolcanic rocks of garnet and amphibolite facies (Dalziel and Brown, 1989). The continent-ward slope of the mountain belt constitutes the Fuegian Cordillera with the main NE verging thrusts complexes. The rocks that crop out here are mainly schists and phyllites of prehnite-pumpellyte to greenschist metamorphic facies (Kohn *et al.*, 1995). The structural style is typical of thick-skinned tectonics, involving the basement rocks with polyphase ductile deformation and post-tectonic intrusions. The external province comprises the Magallanes fold-and-thrust belt, which is located north of the Seno Almirantazgo and Fagnano Lake, across the central-north part of Tierra del Fuego Island. Cenozoic sediments of the SW part of the Magallanes foreland basin are the product of thin-skinned tectonics style, including shallow NNE

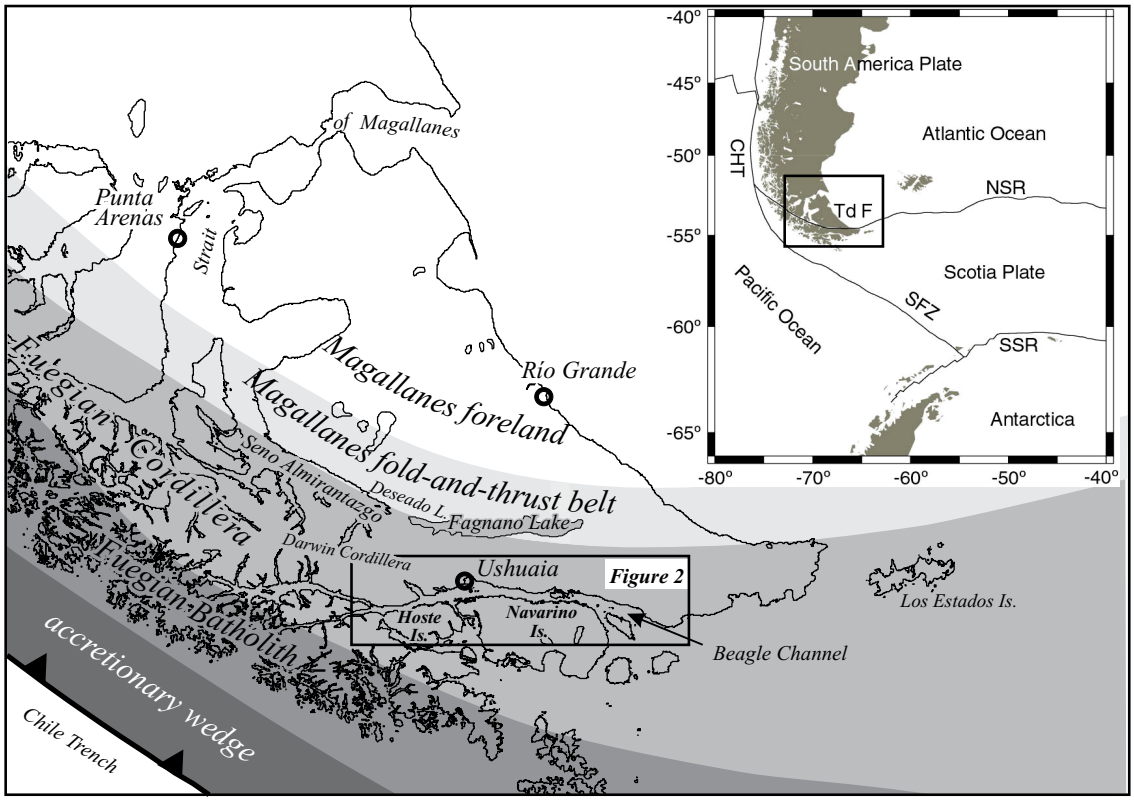

Figure 1. Major morphotectonic provinces in the region of Tierra del Fuego. Inset shows main plates and plate boundaries in the South Atlantic. TdF: Tierra del Fuego; NSR: North Scotia Ridge; SSR: South Scotia Ridge; SFZ: Shackleton Fracture Zone; CHT: Chile Trench.

verging thrust systems. Tight folds with shallow thrusts are stretched in an E-W direction by the Neogene sinistral strike-slip faults, reaching the Atlantic coast. The Fuegian foothills, north of the Tierra del Fuego Island, represent the most external province and are formally included as part of the Magallanes foreland basin; this province is dominated by Neogene terrigenous sediments with slight deformation, involved in large amplitude folds (Menichetti *et al.*, 2008).

The geologic-tectonic arrangement of the Tierra del Fuego island is the product of the long and complex Mesozoic-Cenozoic evolution of southernmost South America, which started with an early Mesozoic active margin of Gondwana stretching between the adjacent southern South America-Antarctic Peninsula and the Pacific margin (Dalziel and Elliot, 1973; Dalziel, 1982). Since Middle Jurassic, the southern part of the continent underwent a widespread extensional phase associated with the breakup of Gondwana; the Jurassic was characterized by crustal melting which resulted in the silicic volcanism of the Large Igneous Province of Patagonia and Antarctic Peninsula (Pankhurst *et al.*, 2000) and the production of oceanic crust in the Rocas Verdes back-arc basin in the southernmost South America (represented by the Tortuga and Sarmiento ophiolitic complexes, Figure 2), and subsequent deposition of quasi-marine sequences (Rocas Verdes assemblages; Dalziel *et al.*, 1974; Bruhn, 1979**;** Dalziel, 1981). Around 100 Ma, a general phase of compressional tectonics led to the closure of the Rocas Verdes basin and the contemporaneous development of the Cordillera and the Magallanes foreland basin, with deposition of clastic sediments sourced in the Cordillera. From late Mesozoic through Tertiary, the Tierra del Fuego region underwent continent-ward propagation of the Magallanes fold-and-thrust-belt (Winslow, 1982; Biddle *et al.*, 1986; Menichetti *et al.*, 2008). This compressive tectonics may have been synchronous with localized strike-slip regime which possibly accommodated the relative motions between South America and the Antarctic continent since Early Cretaceous (Cunningham, 1993, 1995; Peroni *et al*., 2009).

BAHÍA ENSENADA AREA

Bahía Ensenada belongs to the most internal province of the Fuegian Cordillera (Figure 2). Here, the oldest rocks, formally the basement of the chain (Lapataia Formation in Argentine Tierra del Fuego), are exposed in thrust sheets over Jurassic volcanic and sedimentary rocks of Lemaire Formation (Bruhn, 1979; Olivero *et al.*, 1997). The geometry of the structures is related to at least two compressive phases, with folding and thrusting at different structural

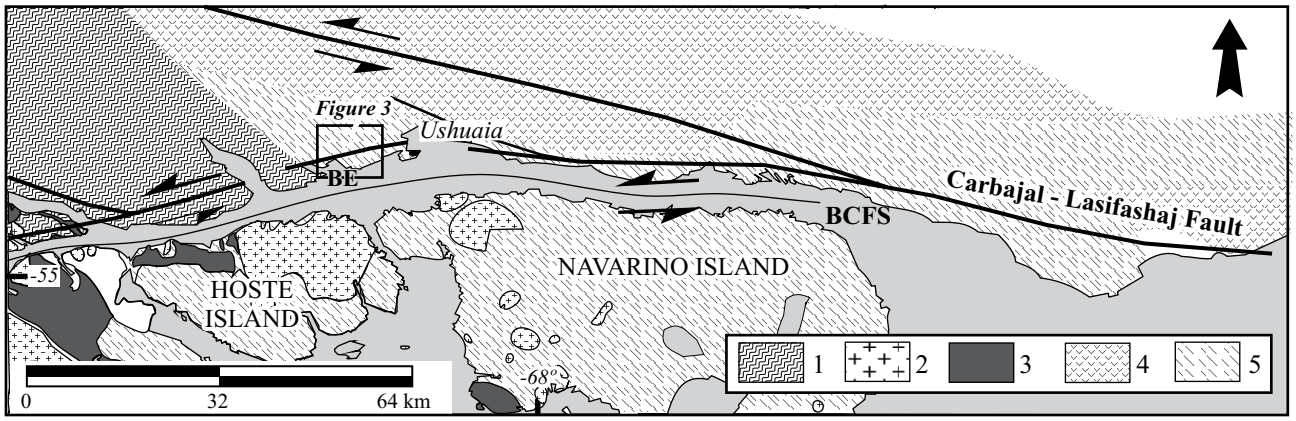

Figure 2. Simplified geological map of the Beagle Channel area. 1: Lapataia Fm.; 2: intrusive bodies of the Fuegian Batholith; 3: Tortuga Complex (basaltic/gabbroic rocks); 4: Lemaire Formation; 5: Yahgán Formation. BCFS: Beagle Channel Fault System; BE: Bahía Ensenada.

levels (Bruhn, 1979), and a third tectonic phase related to a mainly E-W sinistral wrench tectonics, documented in several outcrops along the principal fault systems (Menichetti *et al*., 2004).

The map of Figure 3 displays the main units and structures at Bahía Ensenada area where several hanging wall duplexes of NE-verging thrusts of the Lapataia Formation have moved up relative to the footwall of Jurassic–Cretaceous units (Lemaire and Yahgán formations). These compressive structures in turn are offset by W-E strike-slip faults, likely pertaining to the sinistral Beagle Channel Fault System (Figure 2).

The exposures of the Lapataia Formation are mostly restricted to coastal areas and dominated by fine-grained phyllites displaying polyphase deformation and widespread quartz (± calcite, ± chlorite) veins (Figure 4). Phyllites are banded with quartz-feldspar-rich millimeter to centimeter-layers (Q domains) alternating with phyllosilicate-rich bands (M domains); typical facies variations are related to the Q/M ratio and the abundance of veins. Where Q domains dominate over M domains, phyllites are characterized by ductile folds whereas more brittle, box fold morphologies dominate in M>Q phyllites (Cerredo *et al*., 2006).

The polyphase evolution of Lapataia Formation comprises an early slaty cleavage (S_1) followed by the development of large D_2 folds with a well developed crenulation cleavage. D_2 structures are associated with the formation and emplacement of NE verging fold-and-thrust systems. The slaty cleavage shows a dominant NW-SE trend and dips at high angle either towards S and N-NE (Figure 3a). The main phase fold hinges (F_1) trend from E-W to NW-SE with axial planes generally dipping 40º–60º southwards. The crenulation cleavage has a NW-SE trend dipping towards SW at a higher angle. Three generations of widespread quartz (±calcite, ±chlorite) veins distinguish Lapataia Formation from younger units: the first one is a few millimeters thin, parallel to the S_1 slaty cleavage and is involved in the D_1 centimeter-scale folds and in the metric-scale D_2 folding; the second is a cross-system, a few centimeters thick, subperpendicular to the slaty cleavage and contains the axial plane of the D_2 folds. The trend of such extensional veins is respectively N-S and E-W; a further sub-vertical system with a size of a few centimeters, has a NW-SE trend. All the quartz veins were involved in the younger thrust and normal fault deformations and indicate the large presence of fluids during the development and the propagation of the main Andean phase structures (Menichetti *et al.*, 2004).

Good exposures of Lemaire Formation are found along Bahía Ensenada shoreline (Figures 2 and 3); on the contrary, outcrops in the forest are scarce and discontinuous. The lithological assemblage is composed of a pile of quartz porphyries, silicic breccias and tuffs, tuffaceous schists with interlayered chert horizons and slates, all of which were assigned to the Lemaire Formation (Olivero *et al.*, 1997). In addition, mafic rocks with oceanic affinities occurring within the siliceous volcaniclastic rocks were interpreted as deformed oceanic crust of the Rocas Verdes backarc basin (Cerredo *et al.*, 2007). The complex volcano-sedimentary association of Lemaire Formation also includes pyrite-bearing black shales (Olivero *et al.*, 1997) which host hydrothermal chert horizons at Monte Susana (Ametrano *et al.*, 1999).

The silicic Lemaire rocks have been transformed into light-grey phyllites with relic quartz and feldspar phenocrysts immersed in a totally recrystallized mass of oriented sericite/muscovite, quartz, minor chlorite, occasionally accompanied by unoriented stilpnomelane (Caminos *et al.*, 1981; Olivero *et al.*, 1997). The remnants of oceanic crust, in turn, underwent sea-floor metamorphism (of greenschist and amphibolite facies) later variably modified by Andean compression characterized by very low-grade mineral associations spanning from slightly foliated to mylonitic textures (Cerredo *et al.*, 2007).

The extensive Quaternary glacial deposits, peat and forest in the region make not possible to verify, by direct observation the continuity of geologic formations and

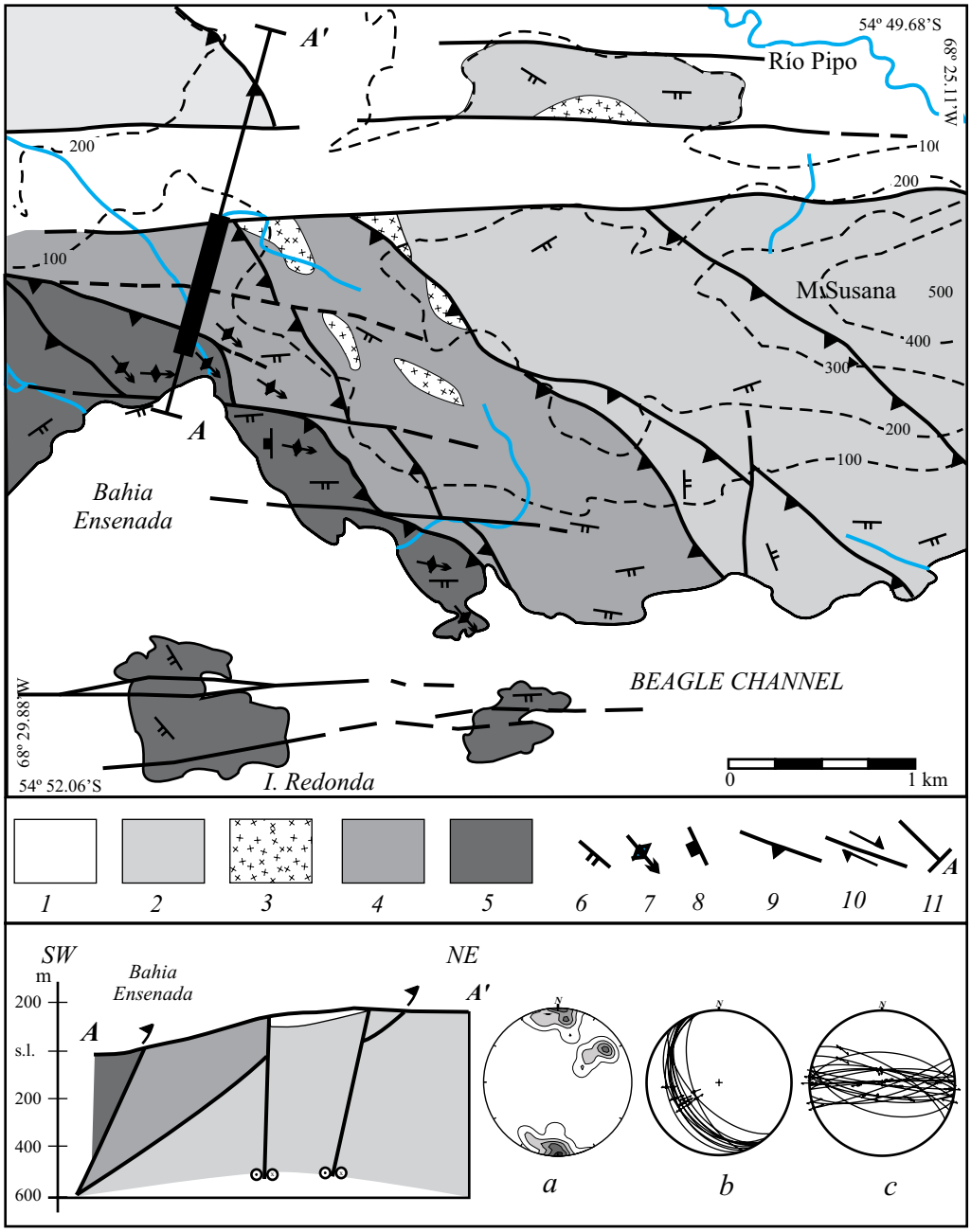

Figure 3. Geological map and cross section of the Bahia Ensenada area. Legend: 1: Quaternary sediments mainly glacial and fluvio-glacial facies; 2: Cretaceous schists of the Yaghan Formation; 3: Upper Jurassic Lemaire Fm, basaltic/gabbroic rocks; 4: Upper Jurassic Lemaire Fm,– siliceous tuffs/ignimbrites; 5: Lapataia Fm; 6: Attitude of slaty cleavage; 7: fold axis; 8: attitude of quartz veins; 9: thrust fault; 10: Strike slip fault; 11: trace of the geological and ERT (thicker line) sections. Lower hemisphere equal area plot of: the slaty cleavage Gaussian contours (k=100) (a); great circles of the thrust planes with slickenlines (b) and strike-slip faults (c).

structures. Therefore, an electric resistivity survey was carried on at Bahía Ensenada, almost perpendicular to the main structures, with the purpose of obtaining a picture of the poorly exposed units in the area and achieving a closer insight into the shallow architecture of the intersection of contractive and strike-slip structures. The ERT survey cuts across Lapataia and Lemaire formations along a slope from the northern Beagle Channel shore in Bahía Ensenada to the lower part of Río Pipo valley (Figure 3).

GEOELECTRIC SURVEY

Data acquisition

Field survey consisted of 1.28 km long geo-electric sounding along the indicated transect in Figure 3, running broadly SSW-NNE almost perpendicular to the main structures. Resistivity measurements were performed with a Syscal R1 resistivity-meter system which operates au-

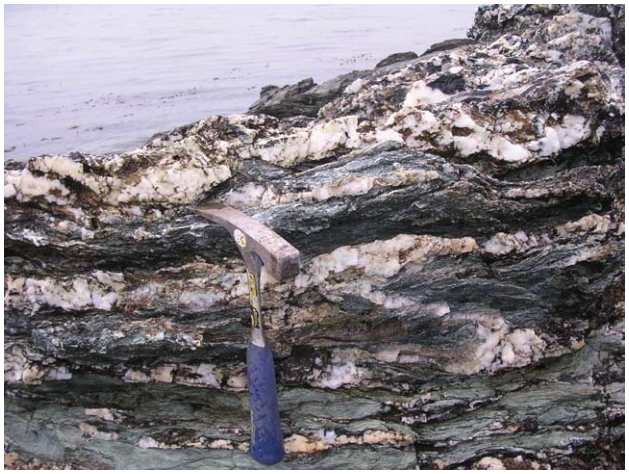

Figure 4. Typical schist of Lapataia Formation at Bahía Ensenada area. Profusion of quartz veins distinguishes this unit from the overlying ones.

tomatically once the geometrical parameters (array type, spacing between electrodes, depth level) are set. For each measurement, the system selects one pair of potential electrodes and one pair of current electrodes with a determined spacing between each quadripole, and automatically records and saves the apparent resistivity value correspondent to the location at pseudo-depth of such measurement.

The resistivity method was applied with a Wenner-Schlumberger array using 48 electrodes connected to a 470 m-long multi-core cable, with four sections and 48 channels. A 470 m long survey was recorded with 48 electrodes, which produced a total number of 546 quadripoles. Time of current injection was 1 s, and a minimum of three and maximum of six repeated measurements at each point was designed in order to obtain a standard deviation <3% for each apparent resistivity value. The minimum spacing between electrodes was set at 10 m for levels 1-5, 20 m for levels 6-8, and 40 m from level 9, so as to ensure better coverage at deepest levels. After completion of measurements for the 470 m long deployed array, partial displacement of the electrodes (12 out of 48) along the profile permitted an extension of the original length (120 meters) and continuous coverage of the subsurface. This procedure, the so called "roll-along method", was repeated several times until 1.28 km of the composite section was reached.

Two-dimensional resistivity tomography provides a resistivity distribution section of a sub-surface portion of the earth from potential measurements made on surface. The basis of a tomography is the pseudosection, which represents the distribution of apparent resistivity measurements taken from electrodes arranged along a line. As depths of investigation are pseudo-depths and resistivities are apparent, the pseudosection offers a qualitative scenario of subsurface resistivity distribution. The characteristics of this distribution depend on the electrode array applied, as well as the true subsurface resistivities. In this way, different electrode arrays can result in quite different pseudosections. There are many electrode configurations, where both potential and current electrodes are arranged along a line with a constant space between adjacent electrodes. These arrays will depend on the geological structures the geophysical method is expected to identify. They are strongly controlled by depth of investigation and their ability to detect vertical and/or horizontal resistivity changes (Loke, 1996-2002). In our case, the Wenner-Shlumberger array was preferred to other arrays as it is sensitive to both horizontal and vertical resistivity variations. Besides better horizontal coverage, the maximum depth of penetration of this array is 15 % larger than the Wenner array (Loke, 1996-2002).

Since the profiling was carried out along a non-horizontal surface, we used differential GPS (acquired by the Astronomic Station of Río Grande, EARG) to account for the topography along the geoelectric transect.

Data processing

Processing of the resistivity pseudosection was accomplished with the RES2DINV program of Geotomo Software (Loke,1996-2002), and included a data filtering phase, and an inversion phase. The filtering phase consisted of the elimination of low quality points, which are characterized by high Q values (>3), being Q the maximum standard deviation measurement. Few points (<5) were eliminated, as the pseudosection presented good quality measurements.

The inversion phase consisted in the application of the smoothness inversion method. This method attempts to find a model (an idealized mathematical representation) of the resistivity distribution of a subsurface section from electric potential measurements made on surface. The 2D model used by the inversion program consists of a number of rectangular blocks (cells). The arrangement of the blocks is loosely tied to the distribution of the data points in the pseudosection and each one of these has its own value of resistivity. The depth of the bottom row of blocks is set to be approximately equal to the equivalent depth of investigation of the data points with the largest electrode spacing. The width of the cells was constrained by the minimum length of the dipoles (10 m) and the thickness of the cells reflects the fact that resolution decreases with depth (the thickness varied from 5 m in the uppermost layer to ~10m for the deepest layer). The software provides the model parameters, which are the resistivity of the cells that better adjusts the values measured at surface. From apparent resistivity measurements (Figure 5a, field pseudosection) the software offers an initial model which predicts a series of calculated apparent resistivity values (Figure 5b, model pseudosection). These values are compared with those obtained from measurements. The comparison of such values allows the model to be modified as many times as the difference between them is below a cutoff value (Loke, 1996-2002). The way the initial model parameters are modified and improved is by solving a least-squares equation, through the smoothness-constrained

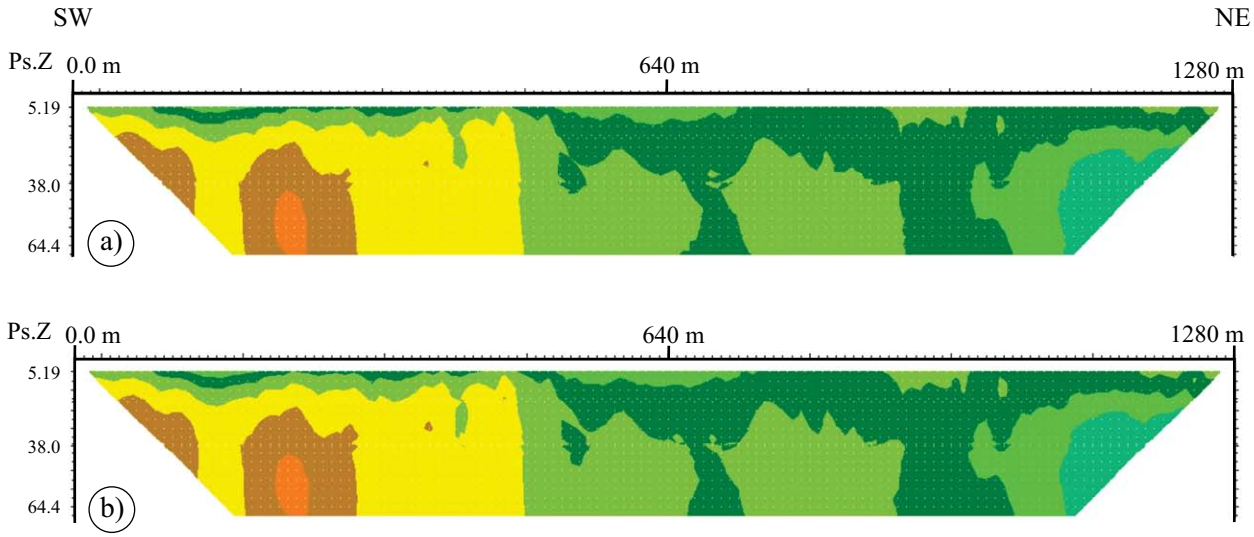

Figure 5. a) Apparent resistivity pseudosection from field measurements (see Figure 3 for location). Wenner-Schlumberger array, unit electrode spacing of 10 m. b) Calculated apparent resistivity pseudosection.

least-squares method (deGroot-Hedlin and Constable, 1990). This method determines the corresponding change in the model parameters that should reduce the sum of squares of the discrepancies between the calculated apparent resistivity values and the apparent resistivity values, and also minimizes the change in the model parameters between iterations. A measure of the difference between calculated values (model data) and apparent resistivity values (field data) is given by the root-mean-squared (RMS) error, which is expressed as percentage.

The method was optimized by applying an algorithm which minimizes the sum of squares of the spatial changes in the model parameters (smoothness-constrained least-squares method with smoothing of model resistivity). Other alternative is the blocky inversion method, in which the sum of absolute values of the discrepancies is reduced. The blocky inversion offers a robust model, where resistivity distribution is quite homogeneous and boundaries within the bodies are sharp. In this work, we preferred the smoothness method as it resulted more representative of subsurface resistivity distribution.

The smoothness constrained inversion method and its optimization finally offered the Electrical Resistivity Tomography of the profile, with a low RMS error of 2.2. It was also possible to incorporate topographic data to the inversion model cells under the option of uniformly distorted grid, where the surface nodes of the mesh match the actual topography. In this option, the nodes below the surface, and thus also the model layers, are shifted to the same extent as the surface nodes (Loke, 1996-2002).

ERT RESULTS AND INTERPRETATION

Figure 6 shows the inversion model and the geological interpretation derived from the ERT analysis. The low RMS error (<3) indicates that the model is accurate; therefore, a reliable interpretation may be drawn from the ERT profile.

The electric tomography, with a modeled maximum penetration depth of ~ 70 m, displays a variation of resistivity values both vertically and horizontally indicating that subsurface rocks are strongly differentiated by their electric properties, according to their lithologies and fracturing degree. Three zones may be distinguished in the ERT section taking into account the distribution of resistivity values (Figure 6a):

Zone 1: The southernmost segment of the profile (0 to ~500 m) is characterized by a strong gradient in resistivity with depth, reaching the highest values recorded on the ERT (~6000 Ω m) at 25 m of depth.

Zone 2: In the central sector of the tomography (from ~500 m to ~900 m) the high resistivity values occur at deeper levels (> 45-50 m) and the region is characterized by low to intermediate resistivities (~200 Ω m) at shallow depths.

Zone 3: The northern portion (from ~900 m to the end of the profile), in turn, shows distinct bodies of intermediate resistivities (~500 Ω m) at very shallow depths set in areas of low to intermediate resistivities (~200 Ω m).

In addition, very low resistivity values (15 – 80 Ω m) were recorded in the northern Zone 1 below -40 m and at the northern ERT section below -30 m which suggest the presence of significant ground water content (water table?).

Resistivity/structure relationships

All along the ERT, significant resistivity lateral variations define a series of sub-vertical and southwest dipping discontinuities which not only separate the three zones described above but also appear within areas of relatively homogeneous resistivity. These thin zones of sharp resistiv-

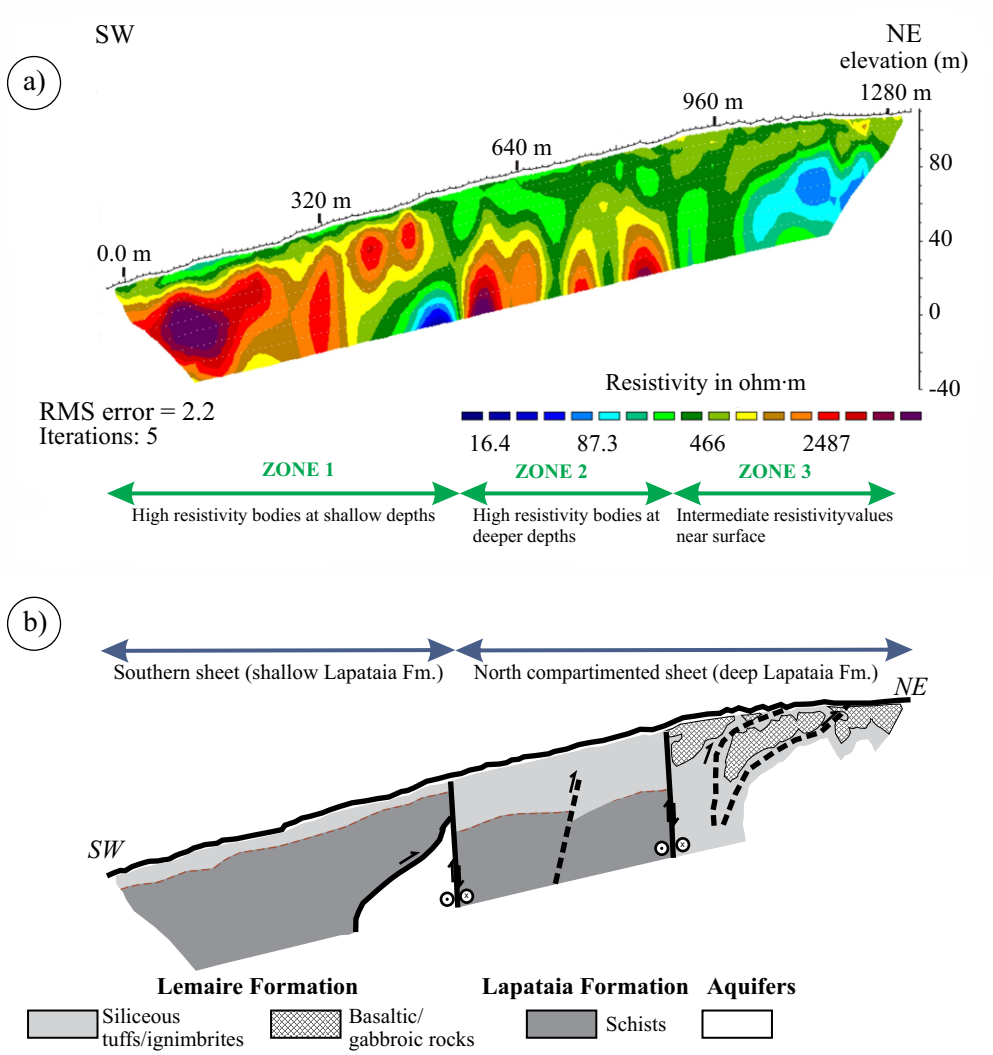

Figure 6. a) Electric resistivity tomography (ERT) section (location in Figure 3) and b) geological interpretation.

ity contrast are interpreted as faults. Generally, fault zones on electrical tomographies are characterized by lower resistivities than the surroundings, due to increased permeability associated with a high density of discontinuities; sharp contrasts in resistivities across discontinuities may also accompany faults on ERT depicting the yuxtaposition of different lithologies (Giocoli *et al*., 2008; Colella *et al.*, 2004; Diaferia *et al*., 2006; Scheibz *et al*., 2009; Suzuki *et al*., 2000).

Two sets of discontinuities may be interpreted from the inversion model of Figure 6a: one with characteristic S-SW, moderate to high angle dip and other fairly vertical. The former are inferred to represent subsurface equivalents of the WNW-ESE trending thrusts (Figure 3).

A conspicuous southwest dipping discontinuity is located at the northern tip of Zone 1 (Figure 6a) and interpreted as a blind thrust plane with no surficial expression. This thrust might be acting as a partial southern barrier to the interpreted water table of Zone 1. Another SW dipping resistivity discontinuity could also be inferred in the subsurface at about 700 m by the sharp lateral resistivity contrast between higher resistivity bodies (2000–6000 Ω m) although not accompanied by clear lithological (resistivity) offsets; other two minor thrusts may be speculated in the northernmost segment of the ERT (Zone 3, Figure 6a). It is noteworthy that the interpreted northern water table would be also partially bounded by the inferred SW dipping thrust plane.

The family of subvertical discontinuities is interpreted as the subsurface expression of the roughly W-E strike-slip mapped structures. A conspicuous resistivity discontinuity is evident in the subsurface at around 900 m in the ERT section in coincidence with the location of the mapped strike-slip fault (Figure 3). The two vertical discontinuities interpreted from the inversion model display a north downthrown block. Although a significant throw of around 15–20 meters may be estimated from the resistivity distribution across the southern fault, this offset should be considered

as the combined throws of the early thrusting and the later transtensive events. The geometries of these faults are observable in several outcrops where subvertical fault planes display left lateral kinematic indicators (*i.e.*, quartz fibers, rock steps and Riedel fractures; Figure 3 b and c)

The general geometric relationships depicted by the inversion model between interpreted thrusts and strike-slip structures indicates that the two styles of deformation are superposed, with the compressive structures being overprinted by wrench tectonism.

Resistivity/lithology relationships

Provided that any type of rock/material is associated with characteristic resistivity ranges (Telford *et al*.,1990; McGinnis and Jensen, 1971; Reynolds and Paren, 1984; Keller and Frishknecht, 1982) which may be also influenced by the degree of fracturing and percentage of fractures filled with groundwater (Loke, 1996-2002), a correlation may be established among domains of relatively homogeneous resistivity and lithology. A summary of the analyzed resistivity data and interpreted lithologies/units are listed in Table 1. The ERT model combined with field data permits clearly to differentiate resistive metamorphic rocks of Lapataia Formation from those less resistive volcano-sedimentary rocks of Lemaire Formation

The characteristic typical profusion of quartz veins in Lapataia Formation (Figure 4) greatly increases its resistivity response given the very low electrical conductivity of quartz. Therefore, the extremely high values (near 6000 Ω m) recorded in the southern sheet at shallow depths and in the southern half of the northern sheet are interpreted as corresponding to Lapataia Formation

The low to intermediate resistivity values forming a thin surficial veneer (~30m) in the southern sheet and a slightly thicker horizon in the southern half of the northern sheet can be assigned to epiclastic, silicic volcanic and volcaniclastic rocks of Lemaire Formation

Well defined elongated bodies of intermediate resistivities at shallow depths are recognized in the northern part of the ERT section. Exposures of mafic rocks close to the ERT section (Figure 3) allow us to assign this intermediate resistivity zones in the subsurface to the mafic facies of Lemaire Formation.

Table 1. Mean electrical resistivity ranges of the geological formations deduced from the ERT model.

Geological Formation	Lithology	Resistivity (Ωm)
Lapataia	Quartz-rich phyllites	2000–6000
Lemaire	Conglomerates, sandstones, tuffs, lapilli	200–450
	Basalts	500–1000

As mentioned before, the lowest resistivity zones appear in two specific locations. According to their resistivity values and shape, they probably correspond to fresh water aquifers confined by south-west dipping discontinuities.

CONCLUSIONS

The electrical resistivity imaging provided significant information of the structural setting of a region characterized by widespread Quaternary cover, peat and forest.

The ERT section allowed recognizing the subsurface continuity of outcropping compressive and wrenching structures as well as the identification of shallow blind structures. This small scale survey confirms the tectonic regional pattern characterized by compressive structures overprinted by transtensional ones.

The subsurface fault plane orientation obtained from ERT images combined with field geology allowed to characterize the thrust planes with SW dipping angles between 25° to 50° (Figure 3, stereonet b) and the W-E oriented strike-slip faults as transtensive subvertical dipping faults belonging to the Beagle Channel Fault System.

Two sheets are interpreted from the ERT section: a southern one with surficial Lemaire Formation overlying Lapataia Formation; and a northern one with a thicker layer of Lemaire Formation displaying internal discontinuities due to transtensive faults and likely minor thrusts.

In the study area Lapataia Formation progressively deepens in a series of thrust duplexes (Figure 3 and 5b), from the southernmost exposed sheet at the Bahía shoreline (not covered by the ERT section), to a shallow location covered by a thin veneer (<20 m) of Lemaire Formation in the southern sheet of the ERT survey. The southern segment of the northern sheet in turn, displays inferred Lapataia Formation below a ~40 m thick Lemaire Formation layer. To the north the transtensive structure which compartments this sheet is inferred to have downthrown the Lapataia Formation below the penetration depth of the ERT survey (>70 m). Therefore the northward stepped deepening of Lapataia Formation is the result of both compressive and transtensive tectonics.

It is noteworthy that inferred minor thrusts within Lemaire Formation are located along the contacts between the mafic and mostly siliceous facies of the unit. Instead, the major thrust of the ERT would not be governed by the contact between Lapataia and Lemaire formations but it cuts across this roughly subhorizontal boundary.

The ERT provided also a closer insight into the relationship between the mafic and the siliceous facies of the Lemaire Formation. The mafic facies occurs as distinct subelliptical bodies, as have been also reported from outcrops elsewhere in central Tierra del Fuego. This characteristic occurrence was interpreted as the product of reshaping of the mafic rocks by Andean compressive tectonics, both at outcrop and in the here interpreted ERT.

The two interpreted aquifers (with characteristic very

low resistivities) are hosted in Lemaire Formation and stalled by faults as they occur confined and bounded by interpreted thrusts and transtensive faults which would be acting as barriers for aquifers.

ACKNOWLEDGMENTS

The authors are very grateful to Ian Dalziel, Vlad Constantin Manea and an anonymous reviewer whose constructive comments improved the original manuscript; the careful editorial revision is also thanked.

We acknowledge those people who contributed to the field work in Tierra del Fuego: Gerardo Connon, Luís Barbero y Carlos Ferrer of the EARG for their support during data acquisition in the field, Parques Nacionales of Argentina by providing facilities for the survey of the National Park of Tierra del Fuego. Augusto Rapalini is thanked for timely and constructive reviews which significantly improved the original manuscript. Funds of this study were partly provided by the CONICET and the Agencia Nacional de Promoción Científica, Tecnológica y de Innovación and the Universidad de Buenos Aires.

REFERENCES

Ametrano, S., Etcheverry, R., Echeveste, H., Godeas, M., Zubia, M. 1999, Depósitos polimetálicos (tipo VMS) en la Cordillera Fueguina, Tierra del Fuego, *en* Zappettini, E.O. (ed.), Recursos Minerales de la República Argentina: Buenos Aires, Argentina, Instituto de Geología y Recursos Minerales, Servicio Geológico Minero Argentino, 35, 1029-1038.

Biddle, K.T., Uliana, M.A., Mitchum, R.M., Fitzgerald, M.G., Wright, R.C., 1986, The stratigraphic and structural evolution of the central and eastern Magallanes Basin, southern South America, *in* Allen, A., Homewood, P. (eds.), Foreland Basins, London, Blackwell Scientific Publications, International Association of Sedimentologists, Special Publication 8, 41-61.

Bruhn, R.L., 1979, Rock structures formed during back-arc basin deformation in the Andes of Tierra del Fuego: Bulletin of the Geological Society of America, 90(11), 998-1012.

Caminos, R., Haller, M., Lapido, J., Lizuain, O., Page, A., Ramos, V., 1981, Reconocimiento geológico de los Andes Fueguinos, Territorio Nacional de Tierra del Fuego, *en* VIII Congreso Geológico Argentino: San Luis, Argentina, 3, 759-786.

Caputo, R., Piscitelli, S., Oliveto, A., Rizzo, E., Lapenna, V., 2003, The use of electrical resistivity tomographies in active tectonics: examples from Tyrnavos Basin, Greece: Journal of Geodynamics, 36(1-2), 19-35.

Caputo, R., Salviulo, L., Piscitelli, S., Loperte, A., 2007, Late Quaternary activity along the Scorciabuoi Fault (Southern Italy) as inferred from electrical resistivity tomographies: Annals of Geophysics, 50(2), 213-223.

Cerredo, M.E., Tassone, A.A., Menichetti, M., 2006, The basement Complex of the Fuegian Andes: microstructures and mineral assemblages*, en* XIII Reunión de Tectónica: San Luis, Argentina, 21.

Cerredo, M.E., Remesal, M.B., Tassone, A., Menichetti, M., 2007, The ocean crust of Rocas Verdes Basin in Tierra del Fuego, Argentina, *en* III Simposio Argentino del Jurásico: Mendoza, Argentina, 33.

Colella, A., Lapenna, V., Rizzo, E., 2004, High-resolution imaging of the high Agri valley basin (Southern Italy) with electrical resistivity tomography: Tectonophysics, 386(1-2), 29–40.

Cunningham, W.D., 1993, Strike-slip Faults in the Southernmost Andes and the development of the Patagonian Orocline: Tectonics, 12(1), 169–186.

Cunningham, W.D., 1995, Orogenesis at the southern tip of the Americas: the structural evolution of the Cordillera Darwin metamorphic complex, southernmost Chile: Tectonophysics, 244(4), 197-229.

Dalziel I.W.D., 1981, Back-arc extension in the southern Andes: a review and a critical reappraisal: Phil. Trans. R. Soc., A., 300, 319-335.

Dalziel, I.W.D., 1982, The early (pre-middle Jurassic) history of the Scotia arc region: a review and progress report, *in* Craddock, C. (ed.), Antarctic Geoscience: Madison, University of Wisconsin Press, 111-126.

Dalziel, I.W.D., Brown, R.L., 1989, Tectonic denudation of the Darwin metamorphic core complex in the Andes of Tierra del Fuego, southernmost Chile: implications for Cordilleran orogenesis: Geology, 17(8), 699-703.

Dalziel, I.W.D., Elliot, D.H., 1973, The Scotia Arc and Antarctic margin, *in* Nairn, A.E.M., Stehli, F.G. (eds.), The Ocean Basin and Margin I: The South Atlantic: New York, Plenum Press, 171-245.

Dalziel, I.W.D., De Wit, M.J., Palmer, K.F., 1974, Fossil marginal basin in the southern Andes: Nature 250(5464), 291-294.

deGroot-Hedlin, C., Constable, S., 1990, Occam´s inversion to generate smooth, two dimensional models for magnetotelluric data: Geophysics, 55(12), 1613-1624.

Demanet, D., Renardy, F., Vanneste, K., Jongmas, D., Camelbeek, T., Megharaoui, M., 2001, The use of geophysical prospecting for imaging active faults in the Roer Graben, Belgium: Geophysics, 66(1), 78-89.

Diaferia, I., Barchi, M., Loddo, M., Schiavone, D., Siniscalchi, A., 2006, Detailed imaging of tectonic structures by multiscale earth resistivity tomographies: The Colfiorito normal faults (central Italy): Geophysical Research Letters, 33(9), L09305.1 - L09305.4.

Fazzito, S.Y., Rapalini, A.E., Cortés, J.M., Terrizzano, C.M., 2009, Characterization of Quaternary Faults by Electric Resistivity Tomography in the Andean Precordillera of Western Argentina: Journal of South American Earth Sciences, 28(3), 217-228.

Giano, S. I., Lapenna, V., Piscitelli, S., Schiattarella, M., 2000, Electrical imaging and self-potencial surveys to study the geological setting of the Quaternary slope deposits in the Agri high valley (Southern Italy): Annali di Geofisica, 43(2), 409-419.

Giocoli, A, Magrì, C., Vannoli, P., Piscitelli, S., Rizzo, E., Siniscalchi, A., Burrato, P., Basso, C., Di Nocera, C., 2008*,* Electrical resistivity tomography investigations in the Ufita Valley (southern Italy): Annals of Geophysics, 51(1), 213-223.

Griffiths, D.H., Barker, R.D., 1993, Two-dimensional resistivity imaging and modelling in areas of complex geology: Journal of Applied Geophysics, 29(3-4), 211-226.

Keller, G.V., Frischknecht, F.C., 1982, Electrical methods in geophysical prospecting: Oxford, Pergamon Press, 519 pp.

Kohn, M.J., Spear, F.S., Harrison, T.M., Dalziel, I.W.D., 1995, 40Ar/39Ar geochronology and P-T-t paths from the Cordillera Darwin metamorphic complex, Tierra del Fuego, Chile: Journal of Metamorphic Geology, 13(2), 251- 270.

Kranck, E.H., 1932, Geological Investigations in the Cordillera of Tierra del Fuego: Acta Geographica, 4(2), 1-231.

Lodolo, E., Menichetti, M., Bartole, R., Ben-Avraham, Z., Tassone, A., Lippai, E., 2003, Magallanes-Fagnano continental transform fault (Tierra del Fuego, southernmost South America): Tectonics, 22(6), 1076, doi: 10.1029/2003TC001500.

Lodolo, E., Lippai, H., Tassone, A., Zanolla, C., Menichetti, M., Hormaechea, J.L., 2007, Morphological and gravity map of the Isla Grande de Tierra del Fuego: Geologica Acta, 5(4), 307-314.

Loke, M.H., 1996-2002, Tutorial: 2-D and 3-D electrical imaging surveys, Geotomo Software.

McGinnis, L.D., Jensen, T.E., 1971, Permafrost-hydrogeologic regimen in

two ice-free valleys, Antarctica, from electrical depth sounding: Quaternary Research, 1(3), 389-409.

Menichetti, M., Acevedo, R., Bujalesky, G., Cenni, M., Cerredo., M.E., Coronato, A., Hormaechea, J.L., Lippai, H., Lodolo, E., Olivero, E., Rabassa, J., Russi., M., Tassone, A., 2004, Field trip guide, Geosur 2004: Argentina, 39 pp.

Menichetti M., Lodolo, E., Tassone, A., 2008, Structural geology of the Fuegian Andes and Magallanes fold-and-thrust belt-Tierra del Fuego Island: Geologica Acta, 6(1), 19-42.

Nivière, B., Bruestle, A., Bertrand, G., Carretier, S., Behrmann, J., Gourry, J.C, 2008, Active tectonics of the southeastern Upper Rhine Graben, Freiburg area (Germany): Quaternary Science Reviews, 27, 541-555.

Nguyen, F., Garambois, S., Chardon, D., Hermitte, D., Bellier, O., Jongmans D., 2007, Subsurface electrical imaging of anisotropic formations affected by a slow active reverse fault, Provence, France: Journal of Applied Geophysics, 62(4), 338-353.

Olivero, E.B., Martinioni, D.R., 2001, A review of the geology of Argentinian Fuegian Andes: Journal of South American Earth Sciences, 14, 175-188.

Olivero, E.B., Acevedo, R.D., Martinioni, D.R., 1997, Geología del Mesozoico de Bahía Ensenada, Tierra del Fuego: Revista de la Asociación Geológica Argentina, 52(2), 169-179.

Pankhurst, R.J., Riley, T.R., Fanning, C.M., Kelley, S.P., 2000, Episodic silicic volcanism in Patagonia and the Antarctic Peninsula: chronology of magmatism associated with the break-up of Gondwana: Journal of Petrology, 41(5), 605–625.

Peroni, J.I., Tassone, A.A., Menichetti, M., Cerredo, M.E., 2009, Geophysical modeling and structure of Ushuaia Pluton, Fuegian Andes, Argentina: Tectonophysics, 476(3-4), 436-449.

Reynolds, J.M., Paren, J.G., 1984, Electrical resistivity of ice from the Antarctic Peninsula: Journal of Glaciology, 30(106), 289–295.

Scheibz, J., Haeusler, H., Kardeis, G., Kohlbeck, F., Chwatal, W., Figdor, H., Koenig, C., 2009, Geologic interpretation of geophysical investigations in the Oslip section, Rust Range, Northern Burgenland, Austria, *in* European Geosciences Union: Vienna, Austria, Geophysical Research Abstracts, 11, 10559.

Spichak V., Fukuoka K., Kobayashi, T., Mogi, T., Popova, I., Shima, H., 2002, ANN reconstruction of geoelectrical parameters of the Minou fault zone by scalar CSAMT data: Journal of Applied Geophysics, 49(1-2), 75-90.

Storz, H., Storz, W., Jacobs, F., 2000, Electrical resistivity tomography to investigate geological structures of the earth's upper crust: Geophysical Prospecting, 48(3), 455-471.

Suárez, M., De La Cruz, R., Bell, C.M., 2000, Timing and origin of deformation along the Patagonian fold and thrust belt: Geological Magazine, 137(4), 345-353.

Suzuki, K., Toda, S., Kusunoki, K., Fujimitsu, Y., Mogi, T., Jomori, A., 2000, Case studies of electrical and electromagnetic methods applied to mapping active faults beneath the thick Quaternary: Engineering Geology, 56(1-2), 29-45.

Tassone, A., Lippai, H., Lodolo, E., Menichetti, M., Comba, A., Hormaechea, J.L., Vilas, J.F., 2005, A geological and geophysical crustal section across the Magallanes-Fagnano fault in Tierra del Fuego and associated asymmetric basins formation: Journal of South American Earth Sciences, 19(1), 99-109.

Telford, W.M., Geldart, L.P., Sheriff, R.E., 1990, Applied Geophysics, Cambridge, United Kingdom, Cambridge University Press, Second Edition, 790 pp.

Winslow, M.A., 1982, The structural evolution of the Magallanes Basin and neotectonics in the southernmost Andes, *in* Craddock, C. (ed.), Antarctic Geoscience: Madison, University of Wisconsin, 143-154.

Wise, D.J., Cassidy, J., Locke, C.A., 2003, Geophysical imaging of the Quaternary Wairoa North Fault, New Zealand: a case study: Journal of Applied Geophysics, 53(1), 1-16.

Manuscript recieved: April 27, 2010
Corrected manuscript received: August 31, 2010
Manuscript accepted: September 4, 2010